Imaging immune response in vivo:

Cytolytic action of genetically altered T-cells directed to glioblastoma multiforme

Jelena Lazovic[1], **Michael C. Jensen**[2], **Evette Ferkassian**[2], **Brenda Aguilar**[2], **Andrew Raubitschek**[3], and **Russell E. Jacobs**[1],*

[1]Biological Imaging Center, Beckman Institute, Division of Biology, California Institute of Technology, Pasadena, California

[2]Division of Molecular Medicine, Beckman Research Institute, Departments of Pediatric Hematology-Oncology, Duarte, California

[3]Radioimmunotherapy, City of Hope National Medical Center, Duarte, California

Abstract

Purpose—Clinical trials have commenced to evaluate the feasibility of targeting malignant gliomas with genetically engineered cytolytic T-cells (CTLs) delivered directly to the tumor bed in the central nervous system (CNS). The objective of this study is to determine a suite of MRI measurements, using an orthotopic xenograft murine model, that can non-invasively monitor immunologically-mediated tumor regression and reactive changes in the surrounding brain parenchyma.

Experimental Design—Our pre-clinical therapeutic platform is based on CTL genetic modification to express a membrane tethered IL13 cytokine chimeric T-cell antigen receptor. This enables selective binding and signal transduction upon encountering the glioma restricted IL-13α2 receptor. We used MRI to visualize immune responses following adoptive transfer of IL13Rα2-specific CD8+ CTL clones.

Results—Based on MRI measurements several phases following IL13Rα2-specific T-cell adoptive transfer could be distinguished, all of which correlated well with glioblastoma regression confirmed upon histology. The first detectable changes, 24 h post treatment, were significantly increased T2-relaxation times and strongly enhanced signal on T1-weighted post-contrast images. In the next phase the apparent diffusion coefficient (ADC) was significantly increased at 2 and 3 days post treatment. In the last phase, at day 3 post IL13Rα2-specific T-cell injection, the volume of hyperintense signal on T1-weighted post contrast image was significantly decreased, while ADC remained elevated.

Conclusions—The present study indicates the feasibility of MRI to visualize different phases of immune response when IL13Rα2-specific CTLs are administered directly to the glioma tumor bed. This will further the aim of better predicting clinical outcome following immunotherapy.

Keywords

Glioblastoma multiforme; Magnetic resonance imaging; immuno therapy; IL-13

INTRODUCTION

Immunotherapy of neoplastic and infectious disease is an area of intense investigation (1-4). As novel immunotherapeutics are applied to clinical trials, the need for reliable non-invasive

*Correspondence should be addressed to: Russell E. Jacobs, Ph.D., M/C 139-74 Caltech, 1200 E. California Blvd., Pasadena, CA 91125-7400. Phone: (626) 395-2849, Fax: (626) 449-5163, rjacobs@caltech.edu

imaging correlates of treatment efficacy and toxicity are imperative for advancing the field. Imaging methods, such as magnetic resonance imaging (MRI), can provide noninvasive longitudinal assessment of a number of tumor characteristics and is a standard modality available to the clinical research community. Measures of these characteristics can be used qualitatively and quantitatively to better predict treatment outcome. Diffusion-weighted MRI (DWI) has been used to evaluate therapeutic responses in a variety of animal tumor models (5-10), and in human clinical studies (11-14). Significantly increased ADC, measured with DWI, in the treated area correlated well with successful treatment and good prognosis, whereas reduced or unchanged ADC correlated with poor treatment and prognosis (5-10). Disrupted blood brain barrier (BBB) permeability is associated with glioblastoma progression, and can be visualized as increased signal intensity on T_1-weighted post contrast MRI (10,15-17). In addition, T_2-weighted MRI provides information about alterations in water mobility thought to be associated with cell death, vasogenic edema and inflammation (18-20). Obtaining multidimensional profiles of tumor response to treatment will significantly facilitate quantitative assessment of treatment efficacy and increase understanding of the underlying mechanism(s), particularly when tumor and therapy generate similar qualitative MRI findings.

Imaging of malignant gliomas presents a particularly challenging venue for imaging antitumor immune responses. We have developed and applied to first-in-human clinical trials for glioblastoma treatment (21,22) a cellular immunotherapy based approach using genetically modified cytolytic T-cells (CTLs) engineered to target interleukin-13 α2 receptor (IL-13Rα2) positive high-grade gliomas including glioblastoma multiforme. These CTLs are modified to express a membrane bound IL-13 cytokine fused to ζ-chain (IL13 - zetakine). *In vitro* studies have shown that activation of the chimeric zetakine receptor upon contact with IL13Rα2$^+$ glioma cells is sufficient to trigger T-cell effector functions ultimately leading to cytolytic destruction of tumor cells (21). A reliable biomarker that can facilitate visualization of interactions between glioblastoma and zetakine expressing CTLs is needed to carefully evaluate *in vivo* applications of this technology and to monitor treatment in the clinical setting.

In this work we explore combined T_2-weighted, DWI and T_1-weighted post contrast MRI in order to determine a reliable suite of measures that correlate well with successful cytotoxic action of zetakine expressing T-cells in a mouse model system. Our focus is on the earliest detectable changes using MRI that prove to have good correlation with final glioblastoma regression. Following successful lysis of glioblastoma cells by IL13Rα2 T-cells we expect an increase in extracellular water content leading to increased water diffusibility due to decreased cell density, and to an increase in transverse relaxation time (T_2). Moreover, it is likely that reversal of disrupted blood brain barrier can indicate successful destruction of glioblastoma cells. We found that increased T_2-relaxation times and strongly enhanced signal on T_1-weighted post contrast images were the first changes, which presented at one day post IL13Rα2 T-cell intracranial injection (i.c.) that correlated well with successful treatment. An increase in ADC (two and three days post) followed; and last was reduction of the volume of hyperintense signal on T_1-weighted post contrast image, three days following IL13Rα2 T-cell i.c. injection.

METHODS

Cell Lines and Cultures

The human glioblastoma cell line U87 was obtained from the American Type Culture Collection (Rockville, MD). Peripheral Blood Mononuclear Cells were obtained from healthy donors participating in a City of Hope National Medical Center Institutional Review Board-approved protocol. The cells were isolated by density gradient centrifugation over Ficoll-Paque (Pharmacia Biotech, Piscataway, NJ). T-cell lines and clones were cultured in RPMI 1640 with 10% heat-inactivated fetal calf serum (FCS), 25 mmol/L HEPES-BSS, 2 mmol/L L-glutamine

and 50 U/mL rhIL-2 (Chiron, Emeryville, CA). Human glioblastoma U87 cells were grown in Dulbecco's Modified Eagle Media supplemented with 10% heat-inactivated FCS, 25 mmol/L HEPES-BSS and 2 mmol/L L-glutamine.

Electroporation of Human T-cells with IL-13 Zetakine cDNA

The IL-13 cDNA synthesis and modification was done according to previously published methods (21). In short, a hygromycin phosphotransferase-HSV thymidine kinase (HyTK) selection/suicide fusion gene under the control of cytomegalovirus immediate-early promoter was inserted into a plasmid containing IL-13 zetakine. The activation of T cells with OKT3 followed by electroporation and subsequent selection in hygromycin/rhIL-2 has been described in more detail previously (23). Cell surface expression of the IL-13-zetakine was assayed by staining with a phycoerythrin-conjugated antihuman IL-13 monoclonal antibody (Becton Dickinson, San Jose, CA) and an IL-13Rα2/hIgG1 chimera (R&D Systems, Minneapolis, MN) detected with a fluorescein isothiocyanate-conjugated antihuman IgG1 monoclonal antibody (Sigma, St. Louis, MO). The phenotype of primary T-cells was determined using fluorescein isothiocyanate-conjugated anti-CD4, and anti-CD8 and anti-TCR α/β monoclonal antibodies (Becton Dickinson, CA).

Orthotopic Glioma Xenograft Model

Male NOD-*scid* mice, 6-8 weeks old were used. Mice were anesthetized with intraperitoneal (*ip*) ketamine/xylazine (132/8.8 mg/kg). The hair on the top of the head was shaved, and prior to incision the head was scrubbed with betadine/alcohol. Mice were immobilized in the stereotaxic restraint apparatus (Stoelting, Wood Dale, IL) and a 5 mm long skin incision was made along the sagital suture. A burr hole was drilled into the skull, 2 mm lateral and 0.5 mm anterior to the bregma, and animals were then transferred to the E15600 Lab Standard Stereotaxic Instrument (Stoelting) for injections using 30-gauge 5 μL Hamilton syringe. Injections were done using a motorized injector over 3 to 5 min. U87-ffLucZeo glioblastoma cells (1×10^5 cells/ μl) were suspended in 2 μL, $1 \times$ PBS (Irvine Scientific, Irvine, CA) and injected bilaterally: 2 mm lateral and 0.5 mm anterior to Bregma; 1 μl was injected at 2.5 mm depth from dura, and 1 μl at 2.25 mm depth from dura. Burr holes were sealed with bone-wax (Ethicon, Inc., Summerfield NJ), and the incisions were closed with Nexaband veterinary glue. To aid in post-surgical recovery, mice were placed on a heating pad and injected with 0.1 mg/kg Buprenex (subcutaneously). All experiments involving the use of animals were performed in accordance with protocols approved by the Animal Care and Use Committee of California Institute of Technology.

Treatment groups

Eleven days following glioblastoma injection N=6 mice were stereotaxically injected with IL-13 zetakine transfected T-cells (3 μl, 2×10^6 cells), N=5 mice were injected with non-specific T-cells (3 μl, 2×10^6 cells), and N=5 mice were injected with PBS (2 μl total volume). The stereotaxic injections were done with the identical coordinates as the original glioblastoma cell injections, with the following exception: IL13Rα2-specific T-cells and non-specific T-cells were injected 1 μL at 2.5 mm depth from dura, 1 μL at 2.35 mm from dura and 1 μL at 2.25 mm from dura.

Magnetic Resonance Imaging

MRI was performed on a 7.0 T Bruker Biospin system using a 2 cm birdcage coil, one day prior (-1 day), and then at one, two and three days post (+1 day, +2 days and +3 days) T-cell/PBS injection. Prior to imaging animals were anesthetized with isoflurane (4% induction, maintenance with 1.5%). During the imaging rectal temperature and respiration were monitored, and isoflurane levels were adjusted if breathing was below 20 BPM or above 40

BPM. The body temperature was maintained between 35-37 °C, during imaging with a custom-built heating solenoid around the body. Each animal was imaged with a T_2-weighted multi-echo spin echo sequence (five 0.5 mm thick slices, TR/TE=3000/10.6-148.4 ms, 14 echoes, 117×117 μm^2 resolution, 4 averages) and diffusion-weighted imaging (five 0.5 mm-thick slices, TR/TE=3000/29 ms, Δ=12 ms, δ=5 ms, with three b-value=0, 500 and 1000 s/mm^2, 127×163 μm^2 resolution, 2 averages). T_1-weighted spin echo (nine 0.5 mm thick slices, TR/TE=500/10.6 ms, 117×117 μm^2 resolution and 8 averages) images were acquired following intravenous (*i.v.*) injection of contrast agent (Magnevist, Berlex Laboratories, Wayne, NJ). After imaging each mouse was recovered on a heating pad, and then returned to his cage. Transverse relaxation time constants (T_2), and ADC were calculated on a pixel-by-pixel basis from the corresponding exponential fits using CCHIPS software (24). Values for the T_2 and ADC histograms were calculated using NIH ImageJ software. Post-contrast hyperintense volumes present in T_1-weighted images (T_1-WI) were determined using an automated segmentation routine, CCHIPS (24). In addition, for animals treated with IL13Rα2 T-cells the analysis of signal intensity on T_1-WI for one day following i.c. injection was done. Upon visual inspection of T_1-WI a strongly enhancing area was observed only in this treatment group one day following i.c. injection. Signal intensity ratios were calculated as: mean signal intensity of the ipsilateral glioblastoma divided by mean signal intensity of the contralateral glioblastoma; mean signal intensity of the strongly enhancing area in the ipsilateral glioblastoma divided by mean signal intensity of the contralateral glioblastoma; and mean signal intensity of the strongly enhancing area in the ipsilateral glioblastoma divided by mean signal intensity of the ipsilateral glioblastoma (leaving out the strongly enhancing part).

Brain Histology and Immunohistochemistry

Four days following T-cell/PBS injections all mice were anesthetized with pentobarbital (100 mg/kg, *i.p.*) and perfused transcardially with 4% paraformaldehyde. The brain tissue was post-fixed overnight in 4% paraformaldehyde and then embedded in paraffin. 10-μm thick sections were cut, deparaffinized and stained by a standard hematoxylin and eosin (H&E) technique. In addition, adjacent slices were processed by heat-induced antigen retrieval procedure using citric buffer (pH 6.0) and then incubated overnight with Mouse monoclonal anti-CD45 (Dako Cytomation, Carpinteria, CA). Sections were processed using Dako EnVision+ systems (peroxidase), with blocking step and secondary antibody dilutions per manufacturer's instructions (Dako Cytomation, Carpinteria, CA). Diaminobenzidine (DakoCytomation) was used as a chromogen. Mayer's hemotoxylin was used for counterstain.

Statistical Analysis

In order to proceed with parametric or non-parametric statistics, data were first confirmed to be normally distributed. Tumor volumes, average T_2 and ADC values within the ipsilateral and contralateral tumor volumes before and after treatment were analyzed using ANOVA with repeated measures. Holm-Sidak method was used for multiple pairwise comparison correction. A *p*-value less then 0.05 was considered statistically significant. Sigma Stat 9.0 (Systat Software Inc., San Hose CA) was used for ANOVA analysis. Histograms for T_2 and ADC values (generated from a single representative slide) prior to and at different days following the same treatment were compared using two-sample Kolmogorov-Smirnov test (*p*-value less then 0.001 was considered statistically significant). Systat 11.0 (Systat Software Inc., San Hose CA) was used for two sample Kolmogorov-Smirnov test.

RESULTS

Changes in transverse relaxation time (T$_2$) following application of IL13Rα2 expressing T-cells

Longitudinal magnetic resonance imaging was used to determine physiological effects associated with IL13Rα2 T-cells, non-specific T-cells and PBS in a murine tumor model system. Variations in the free water content across the tumor and tumor edema can be directly correlated with changes in T$_2$-relaxation time (20). Previously, elevated T$_2$-relaxation times were associated with an increase in extracellular water and decreased cell density (18). Here we expect increased T$_2$-relaxation time as a consequence of glioblastoma cell lysis. Significantly increased T$_2$-values ($p<0.05$) were present in the ipsilateral hemisphere of mice treated with IL13Rα2 T-cells 1 day following the injection (Table 1). This effect is also evident in increased signal on T$_2$-weighted images (Fig. 1). In contrast, there was a significant decrease in T$_2$-relaxation time at the distal tumor site, represented by the contralateral tumor volume, for this treatment group (Table 1). No significant differences were present in mice treated with PBS or non-specific T-cells at any of the imaging times (Fig. 1, Table 1).

In order to examine the variation of T$_2$-values across the tumor, histograms for different days and treatments were calculated (Fig. 1 D-F). Prior to any tumor treatment, all groups had similar T$_2$-distributions (Fig 1 D-F) (Kolmogorov-Smirnov test, $p>0.1$). The earliest change in the histogram distribution, a shift toward longer T$_2$-relaxation times, occurred one day following specific T-cells injections (Fig 1 D, Kolmogorov-Smirnov test, $p<0.001$). For the animals treated with non-specific T-cells there was a significant change in the histogram distribution (Kolmogorov-Smirnov, $p<0.001$) at two and three days following i.c. injections (Fig. 1 E). In contrast to IL13Rα2 T-cell treatment, histograms shifted toward shorter T$_2$-values with non-specific T-cells. There was no significant difference in the histogram distribution for animals treated with PBS at any day following the injection (Kolmogorov-Smirnov, $p>0.001$).

ADC-values changes following application of IL13Rα2 expressing T-cells

Changes in the ADC were used as an additional measurement to detect spatial variations in water mobility and decreased cell density. Increased ADC-values are usually associated with areas of more mobile water (such as extracellular water) and reduced cell density (due to glioblastoma cell lysis) (25). There was no significant change in ADC-values in the first day following any of the treatments. The ADC-values become significantly increased ($p<0.05$) in the ipsilateral glioblastoma treated with IL13Rα2 T-cells at two days following injection (Fig. 2, Table 2), and remained significantly increased the following day (Fig. 2, Table 2). In contrast, no significant increase in ADC-values was detectable in mice injected with PBS or non-specific T-cells at any time point examined (Fig. 2, Table 2).

Histograms were used to evaluate and compare ADC-value distributions within the tumor regions for different days and treatments. Prior to onset of any treatment, all ADC histograms looked similar (Fig. 2 D-F). A significant shift in the ADC distribution toward higher ADC-values occurred only at two and three days following IL13Rα2 T-cell injection (Smirnov-Kolmogorov test, $p<0.001$). There was no significant change in the histogram distributions at any day following PBS or non-specific T-cell injections (Fig. 2 E, F).

Changes in the volume of hyperintense signal on T$_1$-weighted post contrast agent imaging

Increased blood-brain permeability is closely associated with glioblastoma infiltration and progression (15). To investigate the changes in blood-brain barrier properties associated with successful treatment, a series of T$_1$-weighted post-contrast MR imaging studies were performed prior to and at day one and three post treatment. Prior to any treatments there was no significant difference in the volume of hyperintense signal among the various mouse groups

(one-way ANOVA, p>0.3). A tendency toward increased volume of hyperintense signal was noticed at day 1 post injection, independent of treatment group, (Fig. 3 A, B, C, D). A significant decrease in the volume of hyperintense signal was found only 3 days post IL13Rα2 T-cell treatment (Fig. 3 A, B, Table 3).

Histology and correlation with MRI

Basic H&E histology was performed to determine if changes in T_2-relaxation times, ADC-values and volume of hyperintense signals correlate with the successful destruction of glioblastoma. The region with increased T_2-values one day post specific T-cell introduction (Fig. 1) matched closely with the area of highly reduced cell density on H&E (Fig. 4 A, arrowhead). In contrast, reduced cell density was not observed for animals treated with non-specific T-cells or PBS (Fig. 4 B, C). The same area of reduced cell density in H&E stained slides had increased ADC values two and three days post IL13Rα2 T-cells treatment (Fig. 2 and Fig. 4 A). On T_1-weighted images 1 day following IL13Rα2 T-cell injection, a region with strongly enhanced signal could be noted upon visual inspection. This region had significantly increased signal intensity (two sample t-test, $p<0.05$) compared to the remaining ipsilateral glioblastoma, 1.43±0.19 vs. 1.13±0.13, (Fig. 3 A). Signal intensities were normalized to signal intensity in the contralateral glioblastoma. The strongly enhanced region matched very closely the area of glioblastoma regression identified with H&E histology (Fig. 4 A).

To determine the penetration and trafficking of T-cells within the glioblastoma three days following IL13Rα2 or non-specific T-cell injection we used pan-leukocyte marker CD45. T-cells were distributed throughout the tumor for both T-cell types (Fig. 4 D, E). In both cases, T-cells penetrated into the glioblastoma, but did not migrate to the contralateral side (data not shown). However, in the case of non-specific T-cell there was no sign of cytolysis (Fig. 4 E).

DISCUSSION

Several phases of interaction between IL13Rα2 T-cells and glioblastoma cells were revealed by distinct changes observed using multimodal MRI. The initial phase is activation of the antitumor effector function of IL13Rα2 T-cells upon encountering IL13Rα2 positive glioblastoma cells, which occurs within the first 24 h. The earliest detectable changes in this phase are increased T_2-relaxation times and strongly enhancing areas present on the T_1-weighted post contrast images. In the second, lytic phase, massive glioblastoma cell death begins to take place, indicated by an increase in ADC values. In the third, silencing phase, appearance of antigen-specific unresponsive IL13Rα2 T-cells is indicated by a diminished hyper enhancing area in T_1-weighted images, return of T_2-relaxation times to pretreatment values, and continued elevation of ADC values.

Increased T_2-relaxation time indicates presence of antigen reactive T-cells

The initial increase in T_2-relaxation times likely represents strong inflammatory response triggered by specific T-cells encountering IL-13 antigen expressed by the glioblastoma. Similar regional increases in signal intensity on T_2-weighted images were previously reported in animal models of multiple sclerosis (26). Following injection of T-cells specific for myelin basic protein (MBP), areas of the white matter with increased T_2-signal were observed, with the T_2-signal changes attributed to intense inflammation and edema (26). Supporting the hypothesis of strong inflammatory response, one day following application of IL13Rα2 T-cells, is the appearance of an area with strongly enhanced signal intensity on post contrast T_1-weighted image, overlapping with the area of increased T_2-relaxation time. The enhanced regions of white matter on T_1-weighted images following contrast agent injections were also reported for animals injected with T-cells specific for MBP (26). The area with strongly enhanced signal intensity found one day following i.c. IL13Rα2 T-cells is likely the site of

initial antigen reactive IL13Rα2 T-cells, since it overlaps three days later with the area void of contrast enhancement and the area where glioblastoma regression was noted upon histology.

All animals injected with IL13Rα2 T-cells exhibited markedly enhancing white matter tracts on the T_2-weighted image in the ipsilateral hemisphere one day following the injection (Fig. 1). Because this was accompanied by increased ADC values at the same time point, we conclude that this enhancement is due to increased interstitial fluid (brought about by inflammation and edema) along the fibers of the external capsule. The rapid and preferential movement of interstitial fluid along white matter tracts has been reported in rats injected with Evans blue into the frontal region at the grey-white matter junction (27). Increased interstitial fluid may also be a result of glioblastoma cell lysis. However, this is less likely since two days following IL13Rα2 T-cells i.c. injection when ADC become significantly increased, the T_2-enhancement of external capsule is less prominent.

The relatively fast decrease in T2-relaxation times at two and three days following the injection of IL13R□2 T-cells can be attributed to a slow decline in cytotoxic action of T-cells. Alternatively, magnetic susceptibility effects of hemosiderin resulting from the injection may contribute to the reduction of T2-relaxation times. A general trend toward shortening of T2-relaxation times observed in control animals injected with non-specific T-cells and PBS at two and three days post injection supports this explanation. In contrast, a statistically significant decrease of T2-relaxation times in the contralateral glioblastoma of the animals injected with IL13R□2 T-cells, at 1-3 days post injection, is a surprising result, and probably reflects decrease in the glioblastoma extracellular water content, where the exact mechanism is yet to be determined.

Increased ADC, evidence of successful glioblastoma lysis

In accordance with previous studies that used DWI and ADC as markers of therapeutic response in humans and animal models (5-9), we have found good correspondence between tumor regions with increased ADC values and the area of glioblastoma regression identified upon histology. In a recent study utilizing genetically engineered nestin tv-a (Ntv-a) mice, where low and high grade gliomas are developed following infection with ALV-A expressing platelet-derived growth factor (10), increased ADC well correlated with lower grade gliomas, and initial decreased cellularity following temozolomide treatment. A significant increase in ADC was previously reported as early as 24 h following introduction of 1,3-bis(2-chloroethyl)-1-nitrosourea in the rat glioma model (5). While, in this study we observed increased T_2-relaxation times at 24 h i.c. and the earliest detectable increase in ADC was two days following i.c. IL13Rα2 T-cell injection. The difference may be attributed to initial cytotoxic action of T-cells, leading to cytotoxic edema (of glioblastoma cells) and resulting in decreased ADC values. It is possible, however, that the presence of vasogenic edema (noticed as increased T_2-relaxation time, and usually accompanied with increased ADC values) outweighs the effect of cytotoxic edema (reduced ADC values). The simultaneous presence of vasogenic and cytotoxic edema leading to pseudo-normal ADC values has been previously noted in ischemic stroke (28).

Decreased area of signal enhancement on T_1-weighted imaging, beginning of the silencing phase?

The presence of scattered T-cells throughout the tumor was noticed upon histologic examination. However, except for the area that had enhanced MRI signal intensity one day following specific T-cell injection, there was no sign of glioblastoma cytolysis. One possible explanation is antigen-specific T-cell anergy. Rapid development (within six days) of antigen specific anergic T-cells has been observed following specific T-cell adoptive transfer into tumor-bearing host (29). In addition the absence of co-stimulatory factors such as IL-2 may

further accelerate this process (30). A slow decline in cytotoxic activity is further supported by reduction in contrast enhancement, three days following specific T-cell injection.

IL13Rα2 T-cells, MRI and implication for the human studies

Currently, several strategies that employ specific targeting of IL13Rα2 to glioblastoma cells have entered the first or second phase of clinical evaluation (21,31-33). The feasibility and tolerability of IL13Rα2 T-cells are being evaluated in a Food and Drug Administration-authorized pilot study (BB IND#10109). The goal of the pilot study is to evaluate efficacy of IL13Rα2 T-cells delivered to tumor resection cavity following surgery. The main challenge, however, will be development of cytolytic T-cells equipped with factors that can enhance survival and prolong the effector functions in the glioma microenvironment. Development of efficacious methods to monitor tumor response *in vivo* over time will significantly enhance these efforts.

CONCLUSIONS

The ability to predict outcome early in the treatment regime is always desirable, especially with aggressive tumor such as glioblastoma multiforme. Elevated T_2-values at one day, and increased ADC-values at two and three days following IL13Rα2 T-cell injection correlate well with successful cytolytic destruction of glioblastoma by IL13Rα2 expressing T-cells evident on histology. In addition the full or partial restoration of BBB integrity following IL13Rα2 T-cell application is an important MRI indicator of tumor regression. Taken together these indicators provide a powerful measure of tumor response to treatment that can be easily performed in clinical settings to aid better prognosis. In conclusion, longitudinal MRI monitoring provides spatial and temporal discrimination in response of glioblastoma multiforme to IL13Rα2 T-cells in a mouse model system, and aids in establishing early the efficacy of treatment.

Acknowledgements

REFERENCES

1. Liu A, Guardino A, Chinsangaram L, Goldstein MJ, Panicali D, Levy R. Therapeutic vaccination against murine lymphoma by intratumoral injection of recombinant fowlpox virus encoding CD40 ligand. Cancer Res 2007;67:7037–44. [PubMed: 17638917]

2. Porta C, Paglino C, Imarisio I, Bonomi L. Cytokine-based immunotherapy for advanced kidney cancer: past results and future perspectives in the era of molecularly targeted agents. ScientificWorldJournal 2007;7:837–49. [PubMed: 17619768]

3. Sabbatini P, Odunsi K. Immunologic approaches to ovarian cancer treatment. J Clin Oncol 2007;25:2884–93. [PubMed: 17617519]

4. Walden P. Therapeutic vaccination for the treatment of malignant melanoma. Recent Results Cancer Res 2007;176:219–27. [PubMed: 17607929]

5. Hall DE, Moffat BA, Stojanovska J, et al. Therapeutic efficacy of DTI-015 using diffusion magnetic resonance imaging as an early surrogate marker. Clin Cancer Res 2004;10:7852–9. [PubMed: 15585617]

6. Chenevert TL, McKeever PE, Ross BD. Monitoring early response of experimental brain tumors to therapy using diffusion magnetic resonance imaging. Clin Cancer Res 1997;3:1457–66. [PubMed: 9815831]

7. Chenevert TL, Stegman LD, Taylor JM, et al. Diffusion magnetic resonance imaging: an early surrogate marker of therapeutic efficacy in brain tumors. Journal of the National Cancer Institute 2000;92:2029–36. [PubMed: 11121466]

8. Lee KC, Moffat BA, Schott AF, et al. Prospective early response imaging biomarker for neoadjuvant breast cancer chemotherapy. Clin Cancer Res 2007;13:443–50. [PubMed: 17255264]

9. Galons JP, Altbach MI, Paine-Murrieta GD, Taylor CW, Gillies RJ. Early increases in breast tumor xenograft water mobility in response to paclitaxel therapy detected by non-invasive diffusion magnetic resonance imaging. Neoplasia (New York, N.Y 1999;1:113–7.

10. McConville P, Hambardzumyan D, Moody JB, et al. Magnetic resonance imaging determination of tumor grade and early response to temozolomide in a genetically engineered mouse model of glioma. Clin Cancer Res 2007;13:2897–904. [PubMed: 17504989]

11. Di Costanzo A, Trojsi F, Giannatempo GM, et al. Spectroscopic, diffusion and perfusion magnetic resonance imaging at 3.0 Tesla in the delineation of glioblastomas: preliminary results. J Exp Clin Cancer Res 2006;25:383–90. [PubMed: 17167979]

12. Hayashida Y, Hirai T, Morishita S, et al. Diffusion-weighted imaging of metastatic brain tumors: comparison with histologic type and tumor cellularity. Ajnr 2006;27:1419–25. [PubMed: 16908550]

13. Mardor Y, Roth Y, Lidar Z, et al. Monitoring response to convection-enhanced taxol delivery in brain tumor patients using diffusion-weighted magnetic resonance imaging. Cancer research 2001;61:4971–3. [PubMed: 11431326]

14. Mardor Y, Roth Y, Ochershvilli A, et al. Pretreatment prediction of brain tumors' response to radiation therapy using high b-value diffusion-weighted MRI. Neoplasia (New York, N.Y 2004;6:136–42.

15. Cao Y, Nagesh V, Hamstra D, et al. The extent and severity of vascular leakage as evidence of tumor aggressiveness in high-grade gliomas. Cancer research 2006;66:8912–7. [PubMed: 16951209]

16. Oh J, Henry RG, Pirzkall A, et al. Survival analysis in patients with glioblastoma multiforme: predictive value of choline-to-N-acetylaspartate index, apparent diffusion coefficient, and relative cerebral blood volume. J Magn Reson Imaging 2004;19:546–54. [PubMed: 15112303]

17. Leimgruber A, Ostermann S, Yeon EJ, et al. Perfusion and diffusion MRI of glioblastoma progression in a four-year prospective temozolomide clinical trial. International journal of radiation oncology, biology, physics 2006;64:869–75.

18. Valonen PK, Lehtimaki KK, Vaisanen TH, et al. Water diffusion in a rat glioma during ganciclovir-thymidine kinase gene therapy-induced programmed cell death in vivo: correlation with cell density. J Magn Reson Imaging 2004;19:389–96. [PubMed: 15065161]

19. Lazovic J, Basu A, Lin HW, et al. Neuroinflammation and both cytotoxic and vasogenic edema are reduced in interleukin-1 type 1 receptor-deficient mice conferring neuroprotection. Stroke; a journal of cerebral circulation 2005;36:2226–31. [PubMed: 16179572]

20. Oh J, Cha S, Aiken AH, et al. Quantitative apparent diffusion coefficients and T2 relaxation times in characterizing contrast enhancing brain tumors and regions of peritumoral edema. J Magn Reson Imaging 2005;21:701–8. [PubMed: 15906339]

21. Kahlon KS, Brown C, Cooper LJ, Raubitschek A, Forman SJ, Jensen MC. Specific recognition and killing of glioblastoma multiforme by interleukin 13-zetakine redirected cytolytic T cells. Cancer Res 2004;64:9160–6. [PubMed: 15604287]

22. Cooper LJ, Kalos M, DiGiusto D, et al. T-cell genetic modification for re-directed tumor recognition. Cancer Chemother Biol Response Modif 2005;22:293–324. [PubMed: 16110618]

23. Jensen MC, Clarke P, Tan G, et al. Human T lymphocyte genetic modification with naked DNA. Mol Ther 2000;1:49–55. [PubMed: 10933911]

24. Schmithorst VJ, Dardzinski BJ, Holland SK. Simultaneous correction of ghost and geometric distortion artifacts in EPI using a multiecho reference scan. Ieee 2001;Trans Med Imaging 20:535–9.

25. Chenevert TL, Sundgren PC, Ross BD. Diffusion imaging: insight to cell status and cytoarchitecture. Neuroimaging clinics of North America 2006;16:619–32. viii–ix. [PubMed: 17148023]

26. Namer IJ, Steibel J, Poulet P, et al. Blood-brain barrier breakdown in MBP-specific T cell induced experimental allergic encephalomyelitis. A quantitative in vivo MRI study. Brain 1993;116(Pt 1):147–59. [PubMed: 7680933]

27. Geer CP, Grossman SA. Interstitial fluid flow along white matter tracts: a potentially important mechanism for the dissemination of primary brain tumors. Journal of neuro-oncology 1997;32:193–201. [PubMed: 9049880]

28. Ironside, J.; Pickard, J. Raised intracranial pressure, oedema and hydrocephalus. In: Greenfield, JG.; Graham, DI.; Lantos, PL., editors. Greenfield's neuropathology. Vol. 7th ed.. Arnold; London: 2002.

29. Staveley-O'Carroll K, Sotomayor E, Montgomery J, et al. Induction of antigen-specific T cell anergy: An early event in the course of tumor progression. Proceedings of the National Academy of Sciences of the United States of America 1998;95:1178–83. [PubMed: 9448305]

30. Schwartz RH. T cell anergy. Annual review of immunology 2003;21:305–34.

31. Husain SR, Puri RK. Interleukin-13 receptor-directed cytotoxin for malignant glioma therapy: from bench to bedside. Journal of neuro-oncology 2003;65:37–48. [PubMed: 14649884]

32. Kawakami K, Kioi M, Liu Q, Kawakami M, Puri RK. Evidence that IL-13R alpha2 chain in human glioma cells is responsible for the antitumor activity mediated by receptor-directed cytotoxin therapy. J Immunother 2005;28:193–202. [PubMed: 15838375]

33. Kioi M, Husain SR, Croteau D, Kunwar S, Puri RK. Convection-enhanced delivery of interleukin-13 receptor-directed cytotoxin for malignant glioma therapy. Technology in cancer research & treatment 2006;5:239–50. [PubMed: 16700620]
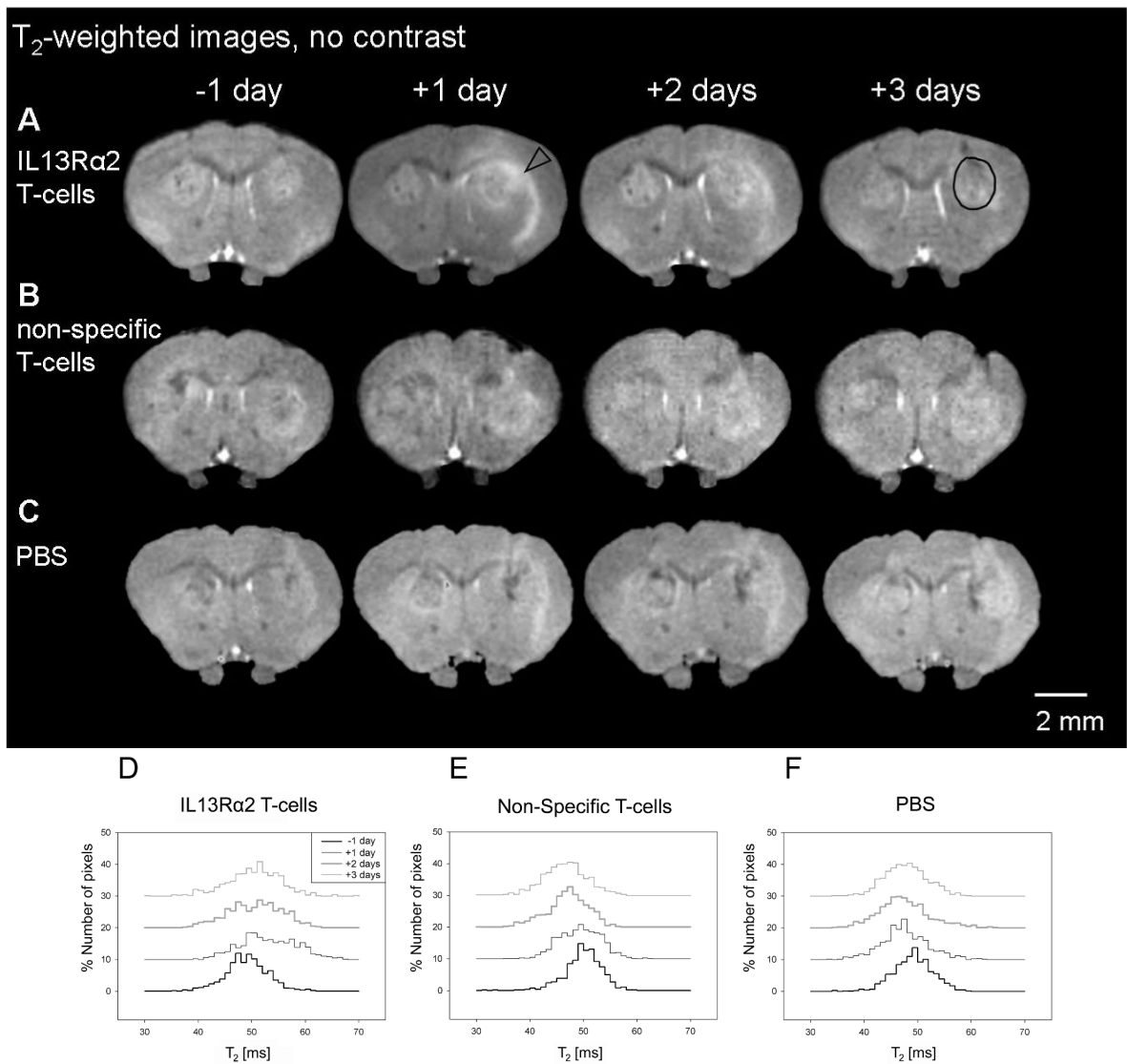
Figure 1. (A-C) Evolution of T$_2$-weighted signal intensity following IL13Rα2 T-cells, non-specific T-cells, PBS and corresponding T2-histograms (D-F)

A single coronal slice of one animal is shown one day prior to treatment and 1-3 days post treatment. Brain slices shown correspond to the level of the anterior commissure. As a consequence of IL13Rα2 T-cell adoptive transfer, increased signal intensity (arrowhead) is observed in the tumor and the external capsule (A). No significant changes were present in animals treated with non-specific T-cells and PBS (B, C). A black circle shows a typical region of interest used for calculating mean T$_2$-relaxation time and T$_2$-histogram distributions. T2-histograms were calculated from a single representative slice using the region of interest from T$_1$-weighted images, and averaged across animals in the each treatment group. One day post i.c. IL13Rα2 T-cell injection, the T$_2$-histogram distribution changes significantly from the distribution prior to treatment with more pixels having increased T$_2$-relaxation times (D). Animals injected with non-specific T-cells had significantly more pixels with shorter T$_2$-relaxation times (E), at 1-2 days post treatment. No significant changes in T$_2$-histogram distribution were present with PBS treatment (F). Two-sample Kolmogorov-Smirnov test, * p<0.001.
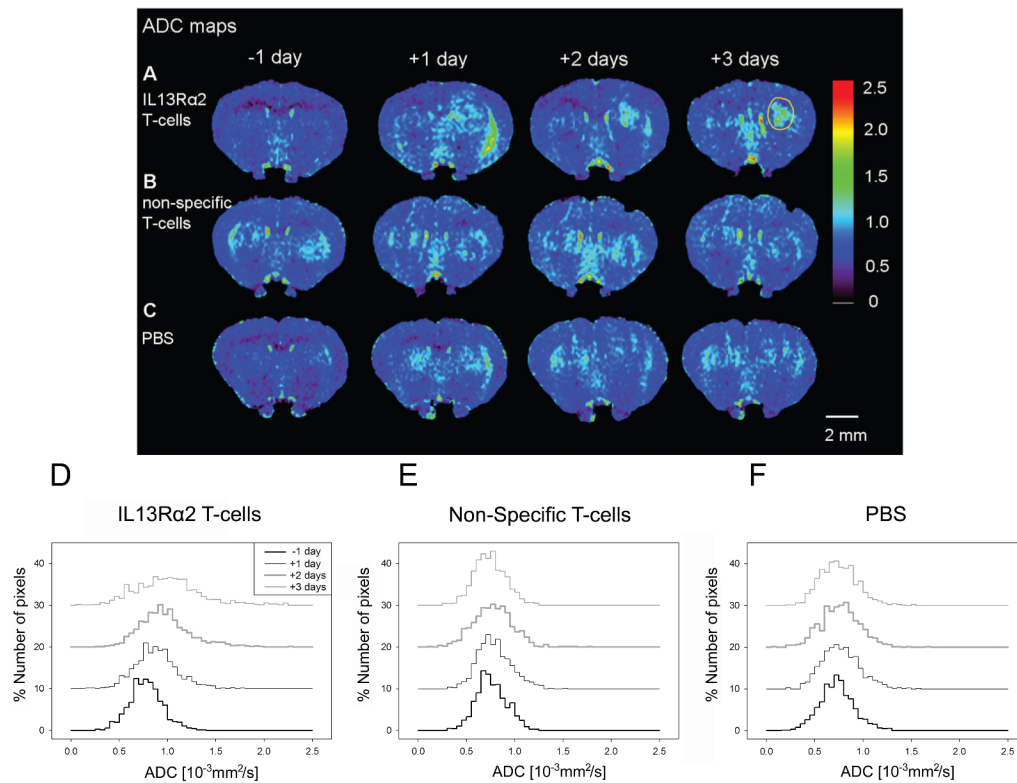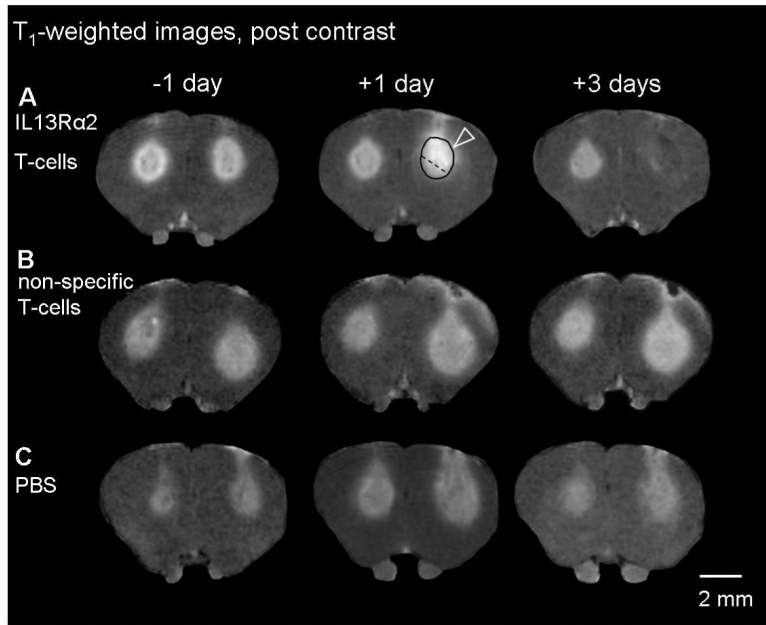
Figure 2. (A-C) Evolution of apparent diffusion coefficient (ADC) following IL13Rα2 T-cells, non-specific T-cells, PBS, and corresponding ADC-histograms (D-F)

A single coronal slice matching the slice position of the T_2-weighted images is shown for one animal at one day prior to and at one, two and three days post corresponding treatment. The ADC values within the glioblastoma became significantly increased at two and three days following IL13Rα2 T-cell adoptive transfer (A). There was no significant increase in ADC values following non-specific T-cell or PBS treatment (B, C). Yellow circle shows a typical region of interest used for calculating mean ADC-values and ADC-histogram distribution. A significant change in ADC-histogram distribution was only present for IL13Rα2 T-cell treated group (D) two and three days post treatment. There were no changes in ADC-histogram distribution for non-specific T-cell (E) or PBS (F) treated animals. Two-sample Kolmogorov-Smirnov test, * $p<0.001$.
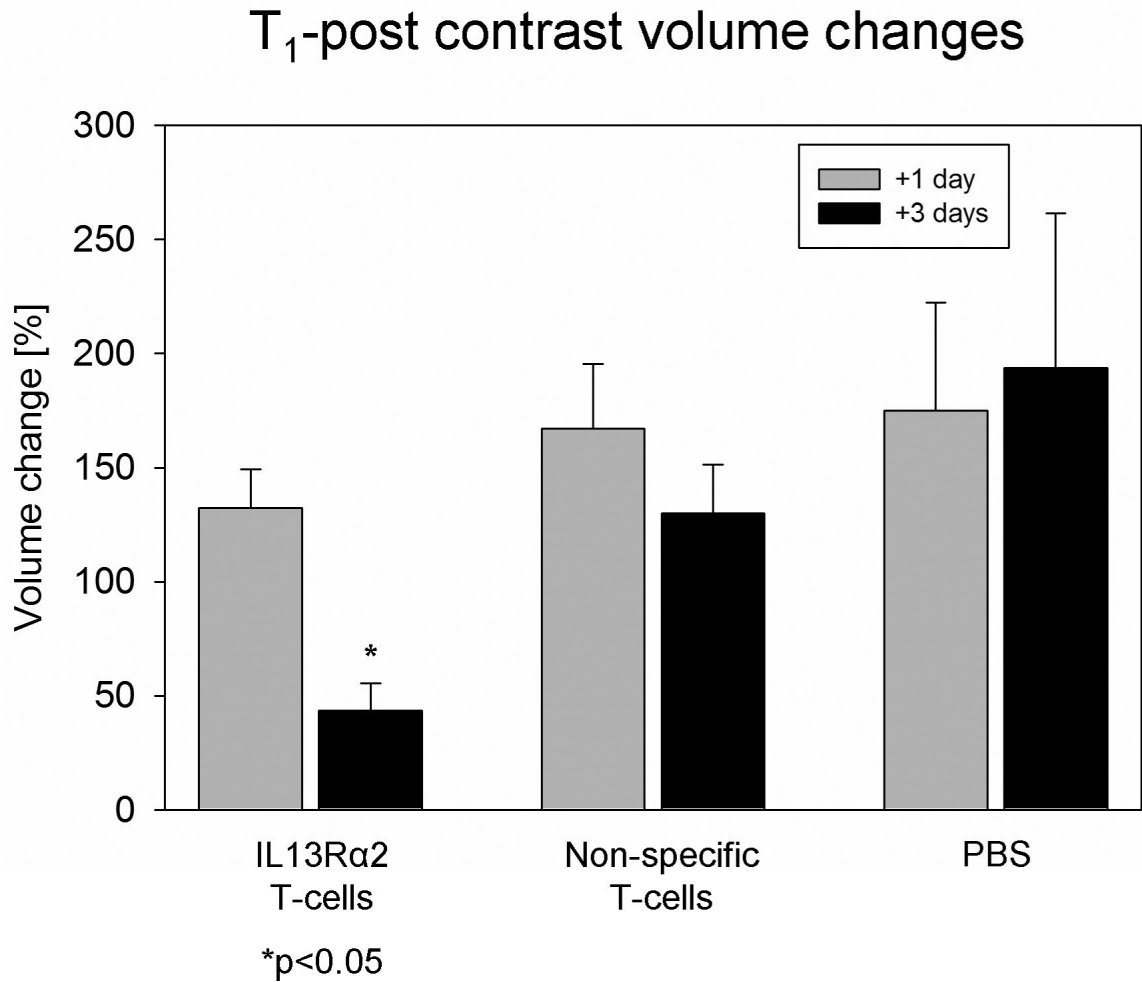
D

Figure 3. (A-C) Evolution of T_1-weighted signal intensity (post contrast) and (D) changes in volume of the signal enhancement, following IL13Rα2 T-cells, non-specific T-cells, PBS
A single coronal slice matching the slice position of the T_2-weighted and ADC images is shown for same animal at one day prior to and at one, and three days post corresponding treatment. Notice a glioblastoma region with significantly increased T_1-weighted signal intensity (arrowhead) at one day following IL13Rα2 T-cell i.c. injection (A). The enhanced signal intensity was not present in this region, three days following IL13Rα2 T-cell injection, indicating glioblastoma regression. There was no significant change in T_1-weighted post contrast signal intensity for animals treated with non-specific T-cell or PBS (B, C). Black circle shows the example of region of interest used for calculating mean signal intensity. A dotted line divides glioblastoma region within strongly enhancing signal intensity from the remaining enhancing area.
(D) All volumes were normalized to the corresponding mean volume one day prior to treatment and expressed as percentage ± SEM of the pretreatment mean volume. ANOVA with repeated measures, with Holm-Sidak correction for multiple pair-wise comparison, * $p < 0.05$.
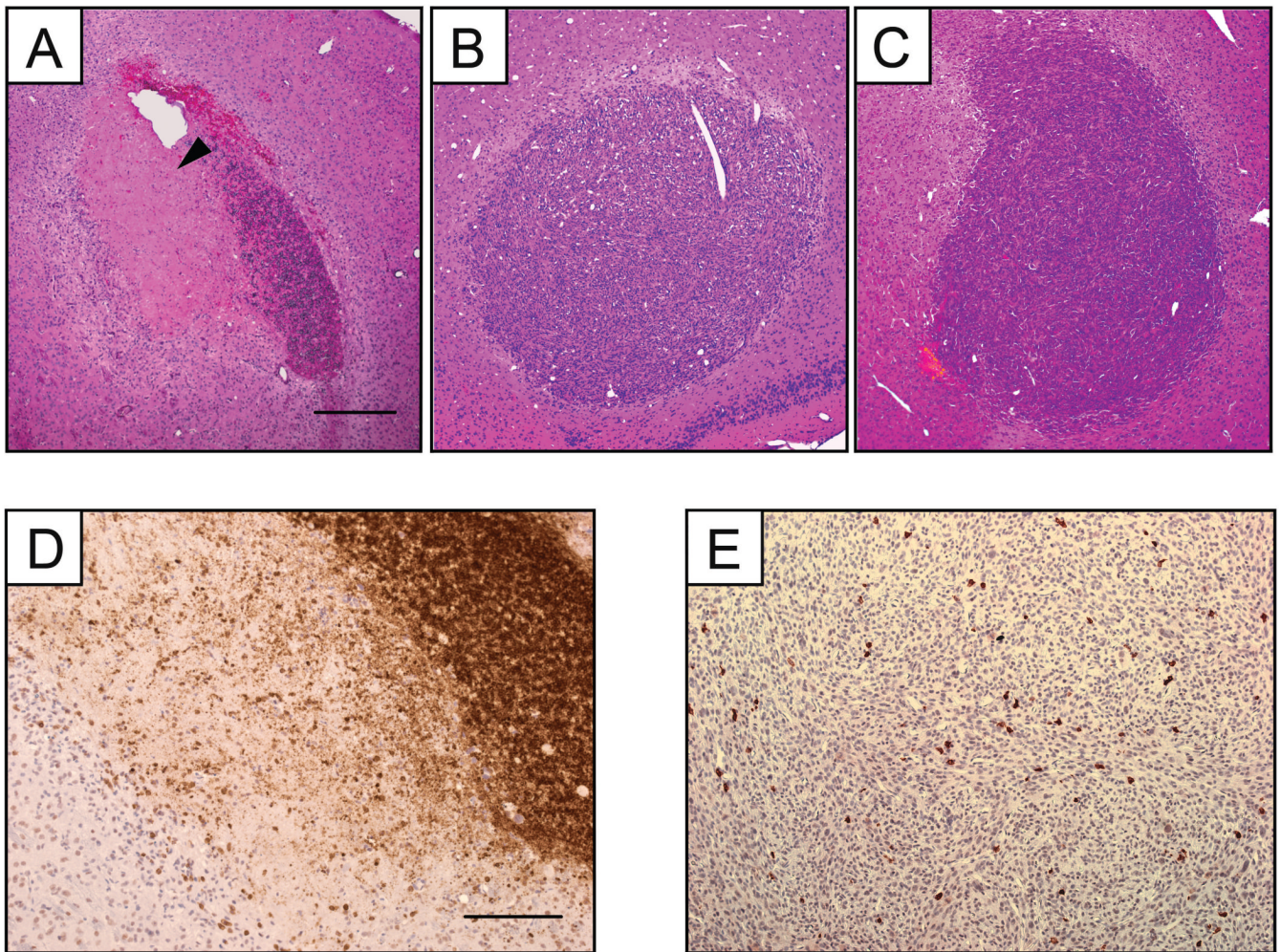
Figure 4. Glioblastoma tumor histology. Hematoxylin and eosin staining of coronal sections corresponding to similar planes of interest in MR images and ADC maps (A-C) and CD-45 staining (D, E)
Ipsilateral side showing glioblastoma regression (arrowhead) in mice treated with IL13Rα2 T-cell (A). Corresponding section of glioblastoma found on ipsilateral side in mice treated with non-specific T-cell (B), and PBS (C) treated mice. Ipsilateral glioblastoma were infiltrated with IL13Rα2 T-cell (D) and non-specific T-cells (E). Scale bar represents 400 μm (A-C), and 200 μm (D, E).

Table 1

Mean T_2-relaxation times for whole tumor volume for different treatment groups and days. Average T_2-values within ipsilateral volumes were calculated for each animal before and compared with after treatment values. The same was done for the contralateral tumor volumes. ANOVA with repeated measures followed by Holm-Sidak post-hoc test was used to determine if the differences in the mean T_2-values among different days of treatment are greater than the differences due to random sampling variability. Results are shown as mean±SD

T_2 [ms]	-1 day	+1 day	+2 days	+3 days
IL13Rα2 T-cells (ipsilateral)	48.5±2.8	52.5±2.3 [*]	50.5±2.7	49.3±2.1
Non-specific T-cells (ipsilateral)	49.8±1.3	48.6±1.9	46.8±2.9	46.0±3.1
PBS (ipsilateral)	48.6±1.1	47.0±2.9	47.0±3.0	47.2±2.6
IL13Rα2 T-cells (contralateral)	49.3±1.6	47.0±2.0 [*]	45.7±1.9 [*]	45.3±2.3 [*]
Non-specific T-cells (contralateral)	48.6±1.5	47.8±2.4	45.6±4.2	45.4±3.3
PBS (contralateral)	46.7±1.3	48.0±3.5	46.2±3.0	47.5±2.1

[*] $p < 0.05$, data is given as mean±SD

Table 2

Mean ADC-values for whole tumor volume for different treatment groups and days. Average ADC-values within ipsilateral tumor volumes were calculated for each animal before and compared with after treatment values. The same was done for contralateral tumor volumes. ANOVA with repeated measures followed by Holm-Sidak post-hoc test was used to determine if the differences in the mean ADC-values among different days of treatment are greater than the differences due to random sampling variability. Results are shown as mean±SD

ADC [$10^{-3}mm^2/s$]	-1 day	+1 day	+2 days	+3 days
IL13Rα2 T-cells (ipsilateral)	7.4±0.6	8.4±0.6	9.4±1.5 [*]	9.7±1.2 [*]
Non-specific T-cells (ipsilateral)	7.2±0.4	7.5±0.3	7.3±0.7	7.0±0.6
PBS (ipsilateral)	6.9±0.3	7.3±0.9	7.2±0.9	7.1±0.7
IL13Rα2 T-cells (contralateral)	7.1±0.7	7.3±0.7	7.2±0.8	6.8±0.6
Non-specific T-cells (contralateral)	7.9±0.8	7.7±0.6	7.5±0.3	6.7±0.3
PBS (contralateral)	6.8±0.5	7.4±1.1	7.1±0.6	7.4±1.3

[*]
p<0.05, data is given as mean±SD

Table 3

Mean tumor volume for different treatment groups and days. Ipsilateral tumor volumes were calculated for each animal before and compared to after treatment volumes. The same was done for contralateral tumor volumes. ANOVA with repeated measures followed by Holm-Sidak post-hoc test was used to compare the mean tumor volumes among same treatment group for different days. Results are shown as mean±SD

T_1-signal volumes [mm^3]	-1 day	+1 day	+3 days
IL13Rα2 T-cells (ipsilateral)	2.82±1.77	3.57±2.17	1.32±1.30[*]
Non-specific T-cells (ipsilateral)	2.26±0.76	3.68±1.40	2.76±0.67
PBS (ipsilateral)	1.67±0.69	2.51±1.06	2.52±0.92
IL13Rα2 T-cells (contralateral)	2.17±0.87	1.57±0.80	2.11±0.77
Non-specific T-cells (contralateral)	2.23±0.37	2.33±0.97	2.08±0.73
PBS (contralateral)	1.34±0.67	1.89±1.14	2.02±1.07

[*] $p < 0.05$, data is given as mean±SD